ehp ENVIRONMENTAL HEALTH PERSPECTIVES
http://www.ehponline.org

Understanding the Radioactive Ingrowth and Decay of Naturally Occurring Radioactive Materials in the Environment: An Analysis of Produced Fluids from the Marcellus Shale

Andrew W. Nelson, Eric S. Eitrheim, Andrew W. Knight, Dustin May, Marinea A. Mehrhoff, Robert Shannon, Robert Litman, William C. Burnett, Tori Z. Forbes, and Michael K. Schultz

http://dx.doi.org/10.1289/ehp.1408855

Received: 21 June 2014
Accepted: 11 March 2015
Advance Publication: 2 April 2015

Understanding the Radioactive Ingrowth and Decay of Naturally Occurring Radioactive Materials in the Environment: An Analysis of Produced Fluids from the Marcellus Shale

Andrew W. Nelson,[1,2] Eric S. Eitrheim,[3] Andrew W. Knight,[3] Dustin May,[2] Marinea A. Mehrhoff,[2] Robert Shannon,[4] Robert Litman,[5] William C. Burnett,[6] Tori Z. Forbes,[3] and Michael K. Schultz[1,7]

[1]Interdisciplinary Human Toxicology Program, University of Iowa, Iowa City, Iowa, USA; [2]University of Iowa State Hygienic Laboratory, Research Park, Coralville, Iowa, USA; [3]Department of Chemistry, University of Iowa, Iowa City, Iowa, USA; [4]Quality Radioanalytical Support, Grand Marais, Minnesota, USA; [5]Radiochemistry Laboratory Basics, The Villages, Florida, USA; [6]Department of Earth, Ocean and Atmospheric Science, Florida State University, Tallahassee, Florida, USA; [7]Department of Radiology and Department of Radiation Oncology, Free Radical and Radiation Biology Program, University of Iowa, Iowa City, Iowa, USA

Address correspondence to Michael K. Schultz, Radiology and Radiation Oncology, University of Iowa, ML B180 FRRB, 500 Newton Road, Iowa City, Iowa 52242 USA. Telephone: +1(319) 335 8017. E-mail: michael-schultz@uiowa.edu

Running title: Radioactivity in shale gas mining waste

Acknowledgments: We kindly acknowledge the staff and faculty at the University of Iowa State Hygienic Laboratory (SHL) for assisting us in this research. Funding for these experiments was provided by the U.S. Nuclear Regulatory Commission (NRC-HQ-12-G-38-0041); and Environmental Management Solutions (Contract EMS FP 07-037-43). R Shannon is employed

by Quality Radioanalytical Support, Grand Marais, Minnesota, USA. R Litman is employed by Radiochemistry Laboratory Basics, The Villages, Florida, USA.

Competing financial interests: MKS is a paid consultant for Speer Law Firm, PA, 104 W 9th Street, Suite 400, Kansas City, Missouri 64105, USA. The other authors declare they have no actual or potential competing financial interests.

Abstract

Background: The economic value of unconventional natural gas resources has stimulated rapid globalization of horizontal drilling and hydraulic fracturing. However, natural radioactivity found in the large volumes of "produced fluids" generated by these technologies is emerging as an international environmental health concern. Current assessments of the radioactivity concentration in liquid wastes focus on a single element – radium. However, the use of radium alone to predict radioactivity concentrations can greatly underestimate total levels.

Objective: We investigated the contribution to radioactivity concentrations from naturally occurring radioactive materials (NORM), including uranium, thorium, actinium, radium, lead, bismuth, and polonium isotopes to the total radioactivity of hydraulic fracturing wastes.

Methods: For this study we used established methods and developed new methods designed to quantitate NORM of public health concern that may be enriched in complex brines from hydraulic fracturing wastes. Specifically, we demonstrate the use of high purity germanium gamma spectrometry and isotope dilution alpha spectrometry to quantitate NORM.

Results: We observed that radium decay products are initially absent from produced fluids due to differences in solubility. However, in systems closed to the release of gaseous radon, our model predicts that decay products will begin to ingrow immediately and (under these closed-system conditions) can contribute to an increase in the total radioactivity for over 100 years.

Conclusions: Accurate predictions of radioactivity concentrations are critical for estimating doses to potentially exposed individuals and the surrounding environment. These predictions must include an understanding of the geochemistry, decay properties, and ingrowth kinetics of radium and its decay product radionuclides.

Introduction

New unconventional-drilling technologies (horizontal drilling combined with hydraulic fracturing, called 'fracking') are unlocking vast reserves of natural gas in the United States and around the world (EIA 2014; Cueto-Felgueroso and Juanes 2013). The potential economic value of these reserves has stimulated a rapid globalization of the approach (Boyer et al. 2011). However the pace of proliferation of these practices has raised concerns about the potential for unintended and undesirable environmental impacts (Finkel 2011; Goldstein et al. 2012; Howarth et al. 2011; Kerr 2010; Schmidt 2011; Thompson 2012). One key environmental issue associated with unconventional drilling and hydraulic fracturing, is the management of water resources and liquid wastes (flowback and produced fluids) (Clark and Veil 2009; Kondash et al. 2013; Lutz et al. 2013; Vidic et al. 2013; Yang et al. 2013; Zhang et al. 2014). Of the environmental contaminants documented in hydraulic fracturing liquid wastes, naturally occurring radioactive materials (NORM) are of particular concern (Brown 2014; Kargbo et al. 2010; Vengosh et al. 2014).

Recent attention has focused on unintentional releases of radium (Ra) isotopes from wastewater treatment plants (Warner et al. 2013), which can arise from incomplete treatment of high ionic strength flowback and produced fluids (Gregory et al. 2011). For example, breakthrough of untreated fluids at a waste treatment facility in central Pennsylvania (northeastern United States) led to Ra contamination in stream sediments measured to be a factor of 200 greater in radioactivity concentration than local background levels (Warner et al. 2013). The magnitude of the Ra contamination at this site prompted the plant operator to proceed with remediation of contaminated sediments in the surface water system (Blacklick Creek) impacted by the discharges (Hunt 2014). Thus, NORM contamination of local environments, arising from

improper treatment and disposal of produced fluids, could emerge as an unintended consequence of hydraulic fracturing. Although, the potential for local populations and workers to experience unhealthy exposures to NORM contained in such wastes is controversial (Brown 2014), monitoring the radioactivity concentrations in these materials is critical to the development of effective waste management strategies and exposure assessments. However, few peer-reviewed reports are available that document levels of NORM in produced fluids. Of those available from the Marcellus Shale (the largest shale-gas formation in the United States), most report radioactivity concentrations of a single element — radium (Barbot et al. 2013; Haluszczak et al. 2013; Nelson et al. 2014; Rowan et al. 2011).

The naturally occurring Ra isotopes of concern (^{226}Ra and ^{228}Ra) have been reported (in peer-reviewed literature) to exceed 670 Bq/L and 95 Bq/L, respectively in produced fluids (Barbot et al. 2013; Haluszczak et al. 2013; Nelson et al. 2014; Rowan et al. 2011). However, little attention has been paid to other environmentally persistent alpha- and beta-emitting NORM, such as uranium (U); thorium (Th); radon (Rn); bismuth (Bi); lead (Pb); and polonium (Po) isotopes (Figure 1). In a review of a report of gross alpha levels in fluids from Marcellus Shale, we observed that reported Ra radioactivity concentrations were similar to maximum gross alpha levels (Barbot et al. 2013), indicating that Ra had been selectively extracted into the liquid wastes, while alpha-emitting daughters remained insoluble under the geochemical conditions of the fluid extraction process. Given that Ra decay products had likely existed in a steady-state radioactive equilibrium with Ra isotopes in the solid shale-formation matrix for millions of years prior to drilling activities, these observations prompted us to explore the radioactive equilibrium relationships of Ra decay products in produced fluids, particularly for the longer-lived alpha-emitters, ^{228}Th ($t_{1/2}$ = 1.91 y) and ^{210}Po ($t_{1/2}$ = 138 d) (half-lives were extracted from NuDat 2

Database [National Nuclear Data Center (NNDC) 2013]).

As we reported previously, the chemical composition of fluids from the Marcellus Shale can interfere with the analysis of Ra isotopes by wet chemistry methods (Nelson et al. 2014). However, the physicochemical properties of select alpha-emitters (^{210}Po, ^{228}Th, and certain U isotopes) allow for chemical extraction and analysis by isotope dilution alpha spectrometry techniques. Thus, we developed a method to analyze alpha-emitting Po, Th, and U isotopes in produced fluids from the Marcellus Shale. Using this method (in systems closed to the release of gaseous radon), we find that estimates of total radioactivity in produced fluids based on Ra isotopes alone can underestimate the total radioactivity present due to the ingrowth of Ra decay-product radionuclides, a process that we demonstrate can be modeled using radioactive ingrowth equations (Bateman 1910). This model predicts that when produced fluids are sealed to the release of radon gas, the total radioactivity concentration of produced fluid can increase by a factor greater than five within the first 15 days following extraction due to the ingrowth of radium decay products. Measurements of decay series radionuclides ^{210}Po and ^{228}Th in produced fluids from the Marcellus Shale presented here support these predictions. Thus, estimates of the radioactivity associated with hydraulic-fracturing liquid wastes must include projections of ingrowth of decay product radionuclides in the natural uranium (^{238}U) and thorium (^{232}Th) decay series.

Methods

General

The State Hygienic Laboratory (SHL) at the University of Iowa is accredited by the United States National Environmental Laboratory Accreditation Program (NELAP). Standard operating procedures and quality assurance measures meet those established by NELAP. All chemical

reagents used were ACS grade or higher. All radioactivity values are decay corrected to the reference date of 7 May, 2013 8:00 a.m. (CST). All uncertainties, unless indicated, are standard uncertainties corresponding to one standard deviation of multiple measurements (Currie 1968).

Tracers and standards

All radioactive tracers were standard Reference Materials (SRMs) obtained from (1) the United States National Institute of Standards and Technology (NIST), (2) NIST-traceable certified reference materials (CRMs) obtained from Eckert & Ziegler Radioisotopes (E&Z) or Analytics or (3) the United Kingdom National Physical Laboratory (NPL) Management Ltd. The following sources were used: a 3 L liquid Marinelli geometry (E&Z 93474), ^{210}Pb (E&Z 94643), ^{nat}U (E&Z CRM 92564), ^{232}U (E&Z CRM 92403 or E&Z 7432; certified in equilibrium with ^{228}Th), ^{230}Th (NIST SRM 4342A or Analytics 67900-294), ^{209}Po (NIST 4326 or E&Z CRM 92565), and multi-line alpha-emitting sources (E&Z 91005, Analytics 59956-121, and Amersham AMR.43).

Sample description

A representative sample of produced fluids from northeastern PA (described previously) was used for all of the following experiments (Nelson et al. 2014). A 200 L drum of Marcellus Shale produced fluids was received at the SHL on May 7, 2013. The sample originated from a well that was horizontally drilled to a depth of 2100 m and fractured with approximately 35,000 m^3 of hydraulic fracturing fluid in early 2012. Analysts at SHL characterized the elemental composition using standard techniques.

High purity germanium (HPGe) gamma spectrometry

HPGe gamma spectrometry of produced fluids was conducted as previously described (Nelson et al. 2014). Briefly, we calibrated our detector to a 3 L liquid Marinelli geometry (E&Z 93474)

using standard practices. To calibrate for the low energy gamma emission of ^{210}Pb, we counted a 3 L Marinelli beaker spiked with ^{210}Pb of known activity (E&Z 94643). This spectrum was merged with the detector calibration using standard features available in ORTEC Gamma Vision (Version 6.08, analysis engine Env32). Quality assurance and quality control (QA/QC) measures included weekly background counts, and linearity and efficiency checks collected three times per week. A 3 L sample was homogenized by heating with 51 g of Bacto Agar (BD 214010) and allowed to cool in a 3 L Marinelli beaker. The sample was then counted for 17 hours on a 30% efficient ORTEC HPGe. Spectral analysis was preformed using ORTEC Gamma Vision (Version 6.08) with a library of radionuclides created in GammaVision Library Editor according to the manufacturer recommendations. All emission energies, half-lives (with exception of ^{209}Po), and their uncertainties were extracted from the NuDat 2 Database [NNDC 2013] and include evaluated nuclear data at of the time of analysis. The sole exception was the half-life of ^{209}Po for which we chose to use 128.3 years (Collé et al. 2007). Data are presented in Table 2.

Alpha-emitting radionuclides

Analysis of produced fluids for alpha-particle emitting radionuclides in the ^{238}U and ^{232}Th decay series (^{210}Po, ^{228}Th, ^{230}Th, ^{234}U, ^{235}U, ^{238}U) was conducted by preconcentration and isotope dilution alpha spectrometry as described below. All results presented are from an unfiltered subsample (20 L, polypropylene carboy) drawn from the homogenized 200 L barrel. The barrel was hermetically sealed following each subsampling for the results reported here. The subsample pH was adjusted to 2 and held (approximately 48 h) to allow iron-rich particulate to dissolve to a transparent, yellowish acidified solution. Pre-concentration and matrix simplification was then conducted via co-precipitation of Po, Th, and U with endogenous iron (Fe) as the hydroxide $Fe(OH)_3$ and added manganese (Mn) for co-precipitation as manganese dioxide (MnO_2), as

previously described (Eichrom 2009; Harada et al. 1989). Preliminary experiments demonstrated exceedingly low concentrations of ^{230}Th, allowing use of ^{230}Th as a radiotracer to determine yields and concentration of ^{228}Th. Following pre-concentration and matrix simplification (via metal oxide/hydroxide co-precipitation; i.e., $Fe(OH)_3$ and MnO_2), Po, U, and Th were separated into radiochemically-pure fractions via extraction chromatography described below.

MnO_2 coprecipitations

Samples were spiked with 150 to 500 mBq of ^{209}Po, ^{230}Th, ^{232}U, ^{nat}U. After appropriate tracers were added, MnO_2 coprecipitations were performed, based on published methods (Burnett et al. 2012; Moore 1976; Nour et al. 2004). $KMnO_4$ (15 or 30 mg) and bromocresol purple (1 mL, 0.1%) were added to acidified (pH < 2) produced fluid (0.5 L) in glass beakers. The sample was diluted twofold (dH_2O), covered with a watch glass, and boiled (1 h). The pH was adjusted to 7-8, the sample was boiled (1 h), and cooled overnight. Following the cooling period, the supernatant was aspirated and the remaining slurry (~50 mL) was transferred to a plastic conical tube (50 mL), centrifuged (10 min), and the supernatant was discarded. Beakers were washed twice (5 mL, 6 M HCl; 1 mL, 1 M ascorbic acid); each time transferring wash to the 50 mL centrifuge tube to dissolve the MnO_2 pellets. Centrifuge tubes were then gently heated in a water bath to fully dissolve pellet and clarify the solution.

Method 1: SR resin and Ag autodeposition separation of polonium

In some cases (see Table 1), Po isotopes were isolated by Eichrom method *Lead-210 and Polonium-210 in Water* (OTW01 Rev. 2.0) (Eichrom 2009). Briefly, samples were spiked with ^{209}Po prior to MnO_2 or $Fe(OH)_3$ precipitation. Precipitates were dissolved (10 mL, 2 M HCl), reduced (1 mL, 1 M ascorbic acid), and gently heated in a water bath. Solutions were then loaded onto preconditioned Eichrom SR Resin (10 mL, 2 M HCl). Columns were rinsed (10 mL, 2 M

HCl) to remove trace contaminants. Po was then eluted with two additions of acid (5 mL, 1 M HNO_3; 15 mL, 0.1 M HNO_3). Eluent was wet ashed (0.5 M HCl) under lower heat with to remove HNO_3. Samples were then dissolved (40 mL, 0.5 M HCl) and reduced (100 mg ascorbic acid). Po was then allowed to autodeposit overnight at 80°C onto silver (Ag) disks painted on one side with acid-resistant acrylic paint. Disks were then cleaned (~10 mL 0.5 M HCl, dH_2O, ethanol, and acetone, in that order) and dried prior to alpha spectrometry.

Method 2: TRU-Ag-TEVA separation (final method)

After MnO_2 coprecipitation and solubilization, most samples (see Table 1) were loaded onto preconditioned TRU cartridges (10 mL, 4 M HCl) to adhere Po, U and Th (Horwitz et al. 1993). TRU resin was washed three times (5 mL, 4 M HCl) before eluting Po, U, and Th (10 mL, 0.1 M ammonium bioxalate) into 150 mL glass beakers containing approximately 20 mL of 0.1 M HCl. The eluent was then reduced to prevent interferences from iron (0.5 mL, 20% w/v hydroxylamine•HCl; 0.1 mL, 1 M ascorbic) (Manickam et al. 2010). Samples were incubated (90°C) in a double boiler on a stir plate. A magnetic stir bar and a polished Ag disk (one side coated with acid-resistant acrylic spray-paint) were placed into the beaker. After 2.5 h, disks were removed and washed (10 mL each 0.1 M HCl, H_2O, ethanol, and acetone, in that order). The remaining solution was taken to dryness and resuspended (10 mL, 4 M HCl). U and Th were then separated on TEVA using a method developed in our laboratory (Knight et al. 2014). The solution of 4 M HCl containing U and Th was loaded onto a preconditioned TEVA column (10 mL, 4 M HCl). Th does not adhere to the column in these conditions. Therefore, Th was collected in the eluent of the load solution along with an additional column wash (10 mL, 4 M HCl). The column was then washed (25 mL, 4 M HCl) to remove trace Th before U was eluted (5 mL, 0.1 M HCl). Th was precipitated by a rare-earth hydroxide as follows: cerium (Ce, 30

μg), bromocresol purple (1 mL, 0.1%), and H_2O_2 (30 μL, 30%). The pH was adjusted to 7 with ammonium hydroxide and left undisturbed (30 min). U sources were prepared by a rare-earth fluoride precipitation by addition of Ce (50 μg), titanium trichloride (1 mL), and hydrofluoric acid (1 mL). U and Th samples were filtered on Eichrom Resolve Filters according to manufacturer's recommendation. For workflow schematic, see Supplemental Material, Figure S1.

Method 3: TRU-TEVA for separation of U and Th

Reported activities of U (Table 1) in the produced fluids were determined using a method previously developed in our laboratory (Knight et al. 2014). This method differs only slightly from those described above. The pellets were dissolved in HNO_3 (10 mL, 2 M) and TRU resin was preconditioned and washed with HNO_3 (10 mL, 2 M) *en lieu* of HCl. This method was investigated but abandoned, as it does not allow for analysis of ^{210}Po.

Isotope dilution alpha spectrometry

All alpha sources were quantitated by standard isotope dilution techniques and counted in vacuum controlled α-spectrometers (Alpha Analyst, Canberra or Alpha Ensemble; ORTEC) as previously described (Knight et al. 2014). Briefly, source-to-detector distances were usually 10 mm, corresponding to a counting efficiency of approximately 18-30%. In some instances, the distance was increased to improve resolution. Radiochemical yields were determined by standard protocols using efficiencies calculated with a NIST traceable, multi-line α-spectrometry standard source (E&Z 91005 or Analytics 59956-121). For all samples, thin films were used to prevent daughter recoil contamination of detectors (Inn et al. 2008). Sources were counted for 17 to 200 hours, as necessary. Standard isotope dilution techniques were used to calculate the activity and recoveries of added controls. In samples where ^{232}U and ^{230}Th were used, activity of ^{228}Th

introduced from the ^{232}U tracer was subtracted using yield determinations for Th isotopes calculated by ^{230}Th. QA/QC included blanks (no added tracers) and laboratory control spikes (LCS). Data are presented in Table 1.

Radioactive ingrowth modeling

Radioactive ingrowth was modeled generally according to the Bateman equation (Bateman 1910) and solved in Microsoft Excel. The derivation and formatting of the Bateman equation was obtained from a previously published source (Choppin et al. 2002).

Results

Radiochemical disequilibria and ingrowth

Radiochemical yields for the final methodology were: Po (81±6%); U (63±8%); Th (85±9 %). In this study, the observed concentrations of natural U (^{238}U, ^{235}U, ^{234}U), and Th isotopes (^{234}Th, ^{232}Th, and ^{230}Th) were exceedingly low (< 5 mBq/L). These levels represented less than 0.001% of the ^{226}Ra radioactivity concentration (670 ± 26 Bq/L; 186 keV peak) in this sample of produced fluids described previously (Nelson et al. 2014). Similarly, we found that the radioactivity concentrations of Ra decay products, including ^{228}Th, ^{214}Pb, ^{214}Bi, ^{212}Pb, ^{210}Pb, ^{210}Po, and ^{208}Tl, were initially near detection limits (Figure 2A, 2B, 2C, 2D, Table 1, Table 2). On the other hand, subsequent analysis of the same sample of produced fluids over time revealed an increase in the radioactivity concentration of decay products ^{210}Po and ^{228}Th, which are supported by ^{226}Ra and ^{228}Ra, respectively (Figure 1; Figure 2A, 2B). Importantly, the storage drum was hermetically sealed between subsamplings for analysis of radioactive decay products to prevent the release of gaseous radon. Notably, under these conditions, the observed increase in radioactivity concentration of ^{210}Po and ^{228}Th followed an established radioactive ingrowth model (Bateman equation), which describes the ingrowth of decay products following a

separation (radioactive disequilibrium) of decay products from the parent radionuclide at time zero (t_0). From these observations we developed a theoretical model for the geochemical partitioning of NORM in the Marcellus Shale formation, within the context of hydraulic fracturing and associated waste disposal activities (Figure 3). This model serves as a guide for predicting the partitioning and radioactive ingrowth/decay of NORM in the environment surrounding unconventional drilling and hydraulic fracturing operations, as well as in the waste treatment and disposal setting. Importantly, the ultimate fate and transport of NORM in the surface and subsurface environment is site dependent; depends also on the potential for release of radon gas; and assessment of the ultimate fate and transport of NORM must be examined on an individual site basis.

Discussion

Modeling the partitioning NORM in Marcellus Shale

The partitioning U and Th decay series radionuclides in Marcellus Shale liquid wastes is a function of elemental geochemical behavior — linked with key biogeochemical features of the formation. Like many marine black-shale formations, the Marcellus Shale is an ancient seabed that became enriched in U associated with organic matter (Carter et al. 2011; Kargbo et al. 2010; Swanson 1961). Produced fluids from the Marcellus Shale have characteristically high levels of salts, the origin of which has several explanations (Blauch et al. 2009). There are notably low levels of sulfate (SO_4^{2-}) (Osborn and McIntosh 2010), likely due to microbial processes that produce sulfides (S^{2-}) (Libes 1992). The ionic strength, reducing environment, and low abundance of SO_4^{2-} alter the potential for NORM to solubilize in produced fluids. For example, low levels of SO_4^{2-} and relatively high ionic strength enhance the solubility of Ra, while reducing conditions promote precipitation of geochemical species of reduced U, i.e., U(IV). Radium decay

product radionuclides, such as Pb and Po are also much more particle reactive and less likely to be extracted through the unconventional drilling and hydraulic fracturing process than decay-series parent Ra isotopes. Thus, differences in the speciation of the elements in the natural decay series govern the likely concentration that will be observed in liquid wastes (as they emerge from depth), following an unconventional drilling and hydraulic fracturing event.

^{232}Th Series partitioning

The parent and supporting isotope in the natural Th decay series, ^{232}Th ($t_{1/2}$ = 1.4 x 10^{10} y), is not expected to undergo oxidation/reduction reactions under natural conditions at depth in the formation, but is nonetheless particle reactive and insoluble in environmental waters and brines (Melson et al. 2003). Accordingly, we observed exceedingly low concentrations of ^{232}Th in unfiltered Marcellus Shale produced fluids. However, the decay of ^{232}Th produces highly soluble divalent alkaline earth ^{228}Ra ($t_{1/2}$ = 5.75 y), which has likely been in radioactive secular equilibrium (steady-state) with ^{232}Th for many millions of years (Gonneea et al. 2008). As a result, produced fluids are enriched in ^{228}Ra (relative to ^{232}Th), which is highly soluble in the high-salt-content brines that describe produced fluids. ^{228}Ra decays by beta-emission to short lived ^{228}Ac ($t_{1/2}$ = 6.15 h), which likely forms insoluble complexes and quickly adsorbs to mineral surfaces at depth — and decays rapidly to form highly-insoluble alpha-particle emitting radionuclide ^{228}Th ($t_{1/2}$ = 1.91 years) (Hammond et al. 1988). Similar to other Th isotopes, ^{228}Th is insoluble in interstitial fluids of shale formations, and its concentration is also observed to be low in produced fluids as they emerge from depth. Notably, the large difference in solubility between ^{228}Ra and ^{228}Th gives rise to a chronometer that has the potential to determine the time when fluids were extracted from the Marcellus Shale (for more information, see Supplementary Material, Expanded Methods, Thorium-228 Ingrowth). As ^{228}Th ingrows at a rate related to its

half-life, its decay product ^{224}Ra ($t_{1/2}$ = 3.63 days), rapidly ingrows to steady-state radioactive equilibrium. Rapid ingrowth of ^{224}Ra is followed by a series of short-lived radioactive decay products that ultimately decay to stable ^{208}Pb (Figure 1). Within this series of relatively short-lived decay products, gaseous ^{220}Rn ($t_{1/2}$ = 55.6 s) presents a potential challenge to modeling expected increases in total radioactivity resulting from radioactive ingrowth processes. On the other hand, because the half-life of ^{220}Rn is so short, migration beyond the immediate vicinity of nuclear formation is likely minimal and disequilibrium is not expected. Thus, in this decay series, the modeled-total ^{228}Ra-supported radioactivity concentration in produced fluids has the potential to increase to a maximum within 5 years of extraction from the shale formation, followed by a decrease determined by the half-life of ^{228}Ra ($t_{1/2}$ = 5.75 y) (Figure 4A and 4B). This suggests that inclusion of the ingrowth and decay of ^{228}Ra decay products (particularly ^{228}Th) is important for development of appropriate liquid waste management.

^{238}U series partitioning

Owing to the geologic history and reducing (anoxic) conditions at depth in the Marcellus Shale formation, parent and supporting radionuclide ^{238}U (which, unlike ^{232}Th can be redox active under natural conditions) is likely to be contained in the crystal lattice of minerals or adsorbed to solid phase structures in a reduced highly-insoluble (+4) oxidation state (Swanson 1961) (Figure 1; Figure 3). Thus, geochemical conditions favor adsorption of ^{238}U and decay-product actinides (^{234}Th, ^{234}Pa, and ^{234}U) to interstitial surfaces of surrounding minerals (Figure 1; Figure 3) (Melson et al. 2003), and these radionuclides are likely fixed at depth. In support of these assertions, we observed exceedingly low concentrations of U and Th radionuclides in unfiltered produced fluids from Marcellus Shale (Table 1, Table 2). Analysis of alpha spectra further revealed an apparent enrichment of ^{234}U (relative to ^{238}U) in produced fluids, which can likely be

explained by alpha-recoil processes (Figure 2E and 2F) (Fleischer 1980; Osmond et al. 1983). Further investigations of partitioning among relevant phases (filtered/ultrafiltered aqueous, particulate, and solid) will provide more detailed understanding of the speciation of actinides in unconventional drilling liquid wastes.

In contrast to low solubility of ^{238}U-series actinides in produced fluids, ^{238}U decay-product radionuclide ^{226}Ra ($t_{1/2}$ = 1600 y) is highly soluble in such fluids. Thus, ^{226}Ra becomes enriched in the aqueous phase at depth relative to supporting actinides, with which ^{226}Ra has likely been in secular equilibrium (steady-state) for many millions of years (Gonneea et al. 2008). Decay product radionuclides of ^{226}Ra are concerning due to the long half-life of ^{226}Ra, which ensures natural production (via radioactive ingrowth) of decay products for thousands of years (Figure 4C, 4D, 4E, and 4F). While ^{226}Ra is highly soluble in produced fluids, our observations suggest that ^{226}Ra decay product radionuclides (Figure 1;Figure 3) are relatively insoluble under these conditions and are retained at depth by interactions with mineral phases in the interstitial environment. Although this geochemical behavior results in very low concentration of ^{226}Ra decay products as fluids emerge from depth, the Bateman radioactivity ingrowth equations predict that (in systems closed to the release of gaseous ^{222}Rn) the total ^{226}Ra-supported radioactivity concentration in produced fluids can increase by a factor greater than five (alpha-particle emissions by a factor of approximately four) over a period of 15 days following extraction of produced fluids (Figure 4D). Importantly, radioactive ingrowth will continue for decades as longer-lived isotopes (^{210}Pb, $t_{1/2}$ = 22 y; ^{210}Po, $t_{1/2}$ = 138 d) approach radioactive equilibrium with ^{226}Ra (at a rate related to their own half-lives; Figure 4E). As an example, we compared the Bateman-equation-based radioactivity ingrowth model to the observed radioactivity concentration of alpha-emitting radionuclide ^{210}Po in sequential analyses of

unfiltered-acidified produced fluids from Marcellus Shale that were stored in a hermetically sealed container for several months. The observed increase in radioactivity concentrations of ^{210}Po in this sample followed the predicted ingrowth under the conditions described (Figure 2A). Ingrowth of long-lived radioactive ^{210}Pb and ^{210}Po is important to overall risk assessments in this context because these radionuclides are potentially bioavailable and may accumulate in higher organisms (Bacon et al. 1988; Cherrier et al. 1995; Fisher et al. 1983; Heyraud and Cherry 1983). Thus, the use of ^{226}Ra alone to predict total radioactivity concentration in liquid drilling wastes can underestimate the increase in levels that will occur over time and neglects the potential for the bioaccumulation of alpha- and beta-emitting decay product radionuclides in bacteria, plants, and higher organisms.

Similar to the decay product scenario of Th-series Ra isotope ^{228}Ra, establishing radioactive equilibrium of decay product radionuclides with parent ^{226}Ra is potentially confounded by the presence of a gaseous isotope (i.e., ^{222}Rn, $t_{1/2}$ = 3.82 d) in the decay series. Further, in this case the half-life of ^{222}Rn is sufficiently long to potentially promote migration and separation (disequilibrium) from parent ^{226}Ra in systems that are open to the atmosphere (e.g., containment ponds; Figure 3). In these cases, the modeled concentration of ^{226}Ra decay products will need to include an assessment of ^{222}Rn emanation and decay to accurately portray the total concentration in liquid drilling wastes and the impact of increased ^{222}Rn and decay products to surroundings.

Conclusion

Previous reports that describe the radioactivity concentration in flowback, produced fluids, and other materials associated with unconventional drilling and hydraulic fracturing have focused on one element – Ra. Our projections suggest that in systems closed to the release of gaseous Rn, estimates based solely on ^{226}Ra/^{228}Ra will underestimate the total activity present by a factor

greater than five within 15 days following extraction as Ra decay product radionuclides ingrow. The level of radioactivity (in a closed ^{226}Ra decay product system) will continue to increase and reach a maximum approximately 100 years after extraction (Figure 4F). At this time, when the long-lived ^{210}Pb and its decay products have reached equilibrium with ^{226}Ra, the total radioactivity will have increased by a factor greater than eight. While this projection assumes losses of Rn and other geochemically derived disequilibria are negligible, the physical process of ingrowth begins again at any time of Ra separation (e.g., sulfate treatment at wastewater treatment plants) and the total activity unavoidably increases as decay product radionuclides ingrow. Thus, long-lived, environmentally persistent Ra decay products (^{228}Th, ^{210}Pb, ^{210}Po) should be considered carefully as government regulators and waste handlers assess the potential for radioactive contamination and exposures.

NORM is emerging as a contaminant of concern in hydraulic fracturing/unconventional drilling wastes, yet the extent of the hazard is currently unknown. Sound waste management strategies for both solid and liquid hydraulic fracturing and unconventional drilling waste should consider the dynamic nature of radioactive materials. Methods designed to remove Ra from hydraulic fracturing waste may not remove Ra decay products, as these elements (Ac, Th, Pb, Bi, Po isotopes) have fundamentally different physicochemical properties (Kondash et al. 2013; Zhang et al. 2014). Future studies and risk assessments should include Ra decay products in assessing the potential for environmental contamination in recreational, agricultural, and residential areas, as well as in developing a more detailed understanding of the accumulation of these radionuclides in higher organisms.

References

Bacon MP, Belastock RA, Tecotzky M, Turekian KK, Spencer DW. 1988. Lead-210 and polonium-210 in ocean water profiles of the continental shelf and slope south of New England. Cont Shelf Res 8:841-853.

Barbot E, Vidic NS, Gregory KB, Vidic RD. 2013. Spatial and temporal correlation of water quality parameters of produced waters from Devonian-age shale following hydraulic fracturing. Environ Sci Technol 47:2562-2569.

Bateman H. 1910. The solution of a system of differential equations occurring in the theory of radioactive transformations. Proc Cambridge Philos Soc 15:423-427.

Blauch M, Myers R, Moore T, Lipinski B, Houston N. 2009. Marcellus Shale post-frac flowback waters-where is all the salt coming from and what are the implications? In: Proceedings from the Society of Petroleum Engineers Eastern Regional Meeting, 23-25 September, 2009, Charleston, WV. SPE-125740. doi: 10.2118/125740-MS

Boyer C, Clark B, Jochen V, Lewis R, Miller CK. 2011. Shale gas: A global resource. Oilfield review 23:28-39.

Brown V. 2014. Radionuclides in fracking wastewater: Managing a toxic blend. Environ Health Perspect 122:A50-A55.

Burnett JL, Croudace IW, Warwick PE. 2012. Pre-concentration of short-lived radionuclides using manganese dioxide precipitation from surface waters. J Radioanal Nucl Chem 292:25-28.

Carter KM, Harper JA, Schmid KW, Kostelnik J. 2011. Unconventional natural gas resources in pennsylvania: The backstory of the modern Marcellus Shale play. Environ Geosci 18:217-257.

Cherrier J, Burnett WC, LaRock PA. 1995. Uptake of polonium and sulfur by bacteria. Geomicrobiol J 13:103-115.

Choppin GR, Liljenzin J-O, Rydberg J. 2002. Radiochemistry and nuclear chemistry. 3rd ed. Worburn, MA:Butterworth-Heinemann.

Clark C, Veil J. 2009. Produced water volumes and management practices in the United States. Argonne National Laboratory (ANL) Publication ANL/EVS/R-09/1. Prepared by the Environmental Science Division, Argonne National Laboratory for the U.S. Department of Energy. Available: http://www.evs.anl.gov/publications/doc/ANL_EVS__R09_produced_water_volume_report_2437.pdf [accessed 17 February 2015].

Collé R, Laureano-Perez L, Outola I. 2007. A note on the half-life of ^{209}Po. Appl Radiat Isot 65:728-730.

Cueto-Felgueroso L, Juanes R. 2013. Forecasting long-term gas production from shale. Proc Natl Acad Sci USA 110:19660-19661.

Currie LA. 1968. Limits for qualitative detection and quantitative determination. Application to radiochemistry. Anal Chem 40:586-593.

EIA (US Energy Information Administration). 2014. Annual energy outlook 2014 early release. Available: http://www.eia.gov/forecasts/aeo/er/pdf/0383er%282014%29.pdf [accessed 8 June 2014].

Eichrom Technologies L. July 28, 2009. Analytical procedures: Lead-210 and polonium-210 in water. Available: http://www.eichrom.com/eichrom/radiochem/methods/eichrom/ [accessed 17 February 2015].

Finkel ML. 2011. The rush to drill for natural gas: A public health cautionary tale. Am J Public Health 101:784-785.

Fisher NS, Burns KA, Cherry R, Heyraud M. 1983. Accumulation and cellular distribution of ^{241}Am, ^{210}Po, and ^{210}Pb in two marine algae. Mar Ecol Prog Ser 11:233-237.

Fleischer RL. 1980. Isotopic disequilibrium of uranium: alpha-recoil damage and preferential solution effects. Science 207:979-981.

Goldstein BD, Kriesky J, Pavliakova B. 2012. Missing from the table: Role of the environmental public health community in governmental advisory commissions related to Marcellus Shale drilling. Environ Health Perspect 120:483.

Gonneea ME, Morris PJ, Dulaiova H, Charette MA. 2008. New perspectives on radium behavior within a subterranean estuary. Mar Chem 109:250-267.

Gregory KB, Vidic RD, Dzombak DA. 2011. Water management challenges associated with the production of shale gas by hydraulic fracturing. Elements 7:181-186.

Haluszczak LO, Rose AW, Kump LR. 2013. Geochemical evaluation of flowback brine from Marcellus gas wells in Pennsylvania, USA. Appl Geochem 28:55-61.

Hammond DE, Zukin JG, Ku T-L. 1988. The kinetics of radioisotope exchange between brine and rock in a geothermal system. J Geophys Res: Solid Earth 93:13175-13186.

Harada K, Burnett WC, LaRock PA, Cowart JB. 1989. Polonium in Florida groundwater and its possible relationship to the sulfur cycle and bacteria. Geochim Cosmochim Acta 53:143-150.

Heyraud M, Cherry R. 1983. Correlation of ^{210}Po and ^{210}Pb enrichments in the sea-surface microlayer with neuston biomass. Cont Shelf Res 1:283-293.

Horwitz EP, Chiarizia R, Dietz ML, Diamond H, Nelson DM. 1993. Separation and preconcentration of actinides from acidic media by extraction chromatography. Anal Chim Acta 281:361-372.

Howarth RW, Ingraffea A, Engelder T. 2011. Natural gas: Should fracking stop? Nature 477:271-275.

Hunt S. 2014. Ohio EPA, health officials dismiss radioactive threat from fracking. The Columbus Dispatch (Columbus, OH) January 27.

Kargbo DM, Wilhelm RG, Campbell DJ. 2010. Natural gas plays in the Marcellus Shale: Challenges and potential opportunities. Environ Sci Technol 44:5679-5684.

Kerr RA. 2010. Natural gas from shale bursts onto the scene. Science 328:1624-1626.

Knight AW, Eitrheim ES, Nelson AW, Nelson S, Schultz MK. 2014. A simple-rapid method to separate uranium, thorium, and protactinium for U-series age-dating of materials. J Environ Radioact 134:66-74.

Kondash AJ, Warner NR, Lahav O, Vengosh A. 2013. Radium and barium removal through blending hydraulic fracturing fluids with acid mine drainage. Environ Sci Technol48:1334-1342.

Libes S. 1992. An introduction to marine biogeochemistry. 1st ed. New York: Wiley.

Lutz BD, Lewis AN, Doyle MW. 2013. Generation, transport, and disposal of wastewater associated with Marcellus Shale gas development. Water Resour Res 49:647-656.

Manickam E, Sdraulig S, O'Brien R. 2010. An improved and rapid radiochemical method for the determination of polonium-210 in urine. Aust J Chem 63:38-46.

Melson NH, Haliena BP, Kaplan DI, Barnett MO. 2003. Adsorption of tetravalent thorium by geomedia. Radiochim Acta 12:617-679.

Moore WS. 1976. Sampling ^{228}Ra in the deep ocean. Deep Sea Res Oceanogr Abstr 23:647-651.

Nelson AW, May D, Knight AW, Eitrheim ES, Mehrhoff M, Shannon R, et al. 2014. Matrix complications in the determination of radium levels in hydraulic fracturing flowback water from Marcellus Shale. Environ Sci Technol Lett 1:204-208.

Nour S, El-Sharkawy A, Burnett WC, Horwitz EP. 2004. Radium-228 determination of natural waters via concentration on manganese dioxide and separation using diphonix ion exchange resin. Appl Radiat Isot 61:1173-1178.

NNDC (National Nuclear Data Center). 2013. NuDat 2 database. Available: http://www.nndc.bnl.gov/nudat2/ [accessed 17 February 2015].

Osborn SG, McIntosh JC. 2010. Chemical and isotopic tracers of the contribution of microbial gas in Devonian organic-rich shales and reservoir sandstones, Northern Appalachian basin. Appl Geochem 25:456-471.

Osmond J, Cowart J, Ivanovich M. 1983. Uranium isotopic disequilibrium in ground water as an indicator of anomalies. Intl J Appl Radiat and Isot 34:283-308.

Rowan E, Engle M, Kirby C, Kraemer T. 2011. Radium content of oil-and gas-field produced waters in the Northern Appalachian basin (USA)—summary and discussion of data. US Geological Survey Scientific Investigations Report 2011-5135. Available: http://pubs.usgs.gov/sir/2011/5135/pdf/sir2011-5135.pdf [Accessed 17 February 2015]

Schmidt CW. 2011. Blind rush? Shale gas boom proceeds amid human health questions. Environ Health Perspect 119:a348.

Swanson VE. 1961. Geology and geochemistry of uranium in marine black shales: A review: US Government Printing Office Washington, DC. Available at: http://pubs.usgs.gov/pp/0356c/report.pdf [Accessed 8 June 2014]

Thompson H. 2012. Fracking boom spurs environmental audit. Nature 485:556-557.

Vengosh A, Jackson RB, Warner N, Darrah TH, Kondash A. 2014. A critical review of the risks to water resources from unconventional shale gas development and hydraulic fracturing in the United States. Environ Sci Technol doi:10.1021/es405118y

Vidic RD, Brantley SL, Vandenbossche JM, Yoxtheimer D, Abad JD. 2013. Impact of shale gas development on regional water quality. Science 340:1235009.

Warner NR, Christie CA, Jackson RB, Vengosh A. 2013. Impacts of shale gas wastewater disposal on water quality in western Pennsylvania. Environ Sci Technol 47:11849-11857.

Yang H, Flower RJ, Thompson JR. 2013. Shale-gas plans threaten China's water resources. Science 340:1288.

Zhang T, Gregory K, Hammack RW, Vidic RD. 2014. Co-precipitation of radium with barium and strontium sulfate and its impact on the fate of radium during treatment of produced water from unconventional gas extraction. Environ Sci Technol 48:4596-4603.

Table 1. Alpha spectrometry of produced fluids. Recoveries, activities, and separation method for select radioisotopes.

Isotope	Activity (mBq/L)	Standard Deviation of Activity (mBq/L)[a]	Recovery (%)	Standard Deviation of Recovery (%)[b]	Days[c]	n	Method[d]
^{210}Po	151	3	42	11	21	3	1
	388	12	28	2	50	3	1
	596	10	13	2	70	3	1
	1000	24	84	6	99	4	2
	4130	40	77	5	278	4	2
^{228}Th	5750	140	71	2	66	4	2
	6900	23	87	7	99	4	2
	22020	850	87	9	278	4	2
^{232}U	N/A	N/A	60	3	99	3	2
	N/A	N/A	69	8	278	3	2
^{238}U	1.13	0.17	70	3	28	3	3
^{235}U	0.14	0.05	70	3	28	3	3
^{234}U	2.58	0.88	70	3	28	3	3

[a]Standard deviation of multiple counts. [b]Standard deviation of multiple counts. [c]After 8 a.m. on 7 May 2013 (CST). [d]1 = Sr-Ag Autodeposition, 2 = TRU-Ag-TEVA, 3 = TRU-TEVA.

Table 2. HPGe gamma spectrometry of produced fluids. HPGe analysis of 3 L produced fluids homogenized with BactoAgar in a 3 L Marinelli beaker.

Isotope	Activity (Bq/L)	Uncertainty (Bq/L)[a]	CL (Bq/L)[b,c]	Peaks (keV)
^{228}Ac	76	1	0.6	911, 338
^{224}Ra	21	3	3	241
^{212}Pb	2.4	0.3	0.2	239
^{208}Tl	<CL	N/A	1	860
^{234m}Pa	<CL	N/A	13	1001
^{234}Th	<CL	N/A	7	63
^{226}Ra	670	3	3	186
^{214}Pb	256	2	0.8	295, 242, 580, 480
^{214}Bi	235	1	0.3	609, 1120,1238, 768, 934, 1385, 1583, 274
^{210}Pb	<CL	N/A	20	46
^{40}K	10	1	1	1461

[a]Uncertainties are GammaVision generated counting uncertainties. [b]At time of acquisition 2:18 PM (CST) on 15 May 2013. [c]Critical level (CL) determined by the Currie Limit

Figure Legends

Figure 1. Natural thorium and uranium decay chains. Half-lives and decay information from the NuDat 2 Database [NNDC 2013].

Figure 2. Po, Th, and U activities and alpha spectra. **(A)** Theoretical Bateman model of ^{210}Pb ingrowth (blue) and ^{210}Po (red) given ^{226}Ra levels and a system closed to emanation of gaseous radon in produced fluids sample with our empirical data (black squares, error bars subsumed within boxes). **(B)** Theoretical Bateman model of ^{228}Th ingrowth (green) and ^{228}Ra decay (blue) given ^{228}Ra levels and a system closed to emanation of gaseous radon in produced fluids sample with our empirical data in black (error bars subsumed within boxes). **(C)** Representative Po alpha spectrum of ^{209}Po tracer (orange) and ^{210}Po (red). **(D)** Representative Th alpha spectrum of ^{230}Th tracer (purple), ^{228}Th (green), and ^{228}Th decay products (black). ^{232}Th was virtually undetectable by this method. **(E)** Activities of ^{238}U (purple), ^{235}U (black), and ^{234}U (orange) in produced fluids with error bars representing one standard deviation of the determined activity of multiple counts (n=3). **(F)** Representative U alpha spectrum of ^{238}U (purple), ^{235}U (not labeled), ^{234}U, ^{232}U tracer (blue) and ^{232}U tracer decay products (^{228}Th green, others black).

Figure 3. Partitioning of NORM in Marcellus Shale and associated waste. Theoretical model of NORM partitioning based on HPGe gamma spectrometry and alpha spectrometry of produced fluids. Solid arrows indicate a radioactive decay or series of radioactive decays. Dashed arrows indicate a physical or chemical partitioning process.

Figure 4. Ingrowth of radium decay products. Theoretical Bateman model of Ra decay product ingrowth and decay (system closed to release of gaseous radon). **(A)** 15 days after extraction for ^{228}Ra (green dots), associated alpha (red dashes) and total activity (blue); **(B)** 70 years after extraction for ^{228}Ra (green dots), associated alpha (red dashes) and total activity (blue); **(C)** 70 years after extraction for ^{226}Ra (purple), ^{228}Ra (green dots), associated alpha (red dashes) and total activity (blue); **(D)** 15 days after extraction for ^{226}Ra (purple), associated alpha (red dashes) and total activity (blue); **(E)** 70 years after extraction for ^{226}Ra (purple), associated alpha (red dashes) and total activity (blue); **(F)** 5000 years after extraction for ^{226}Ra (purple), associated alpha (red dashes) and total activity (blue).

Figure 1.

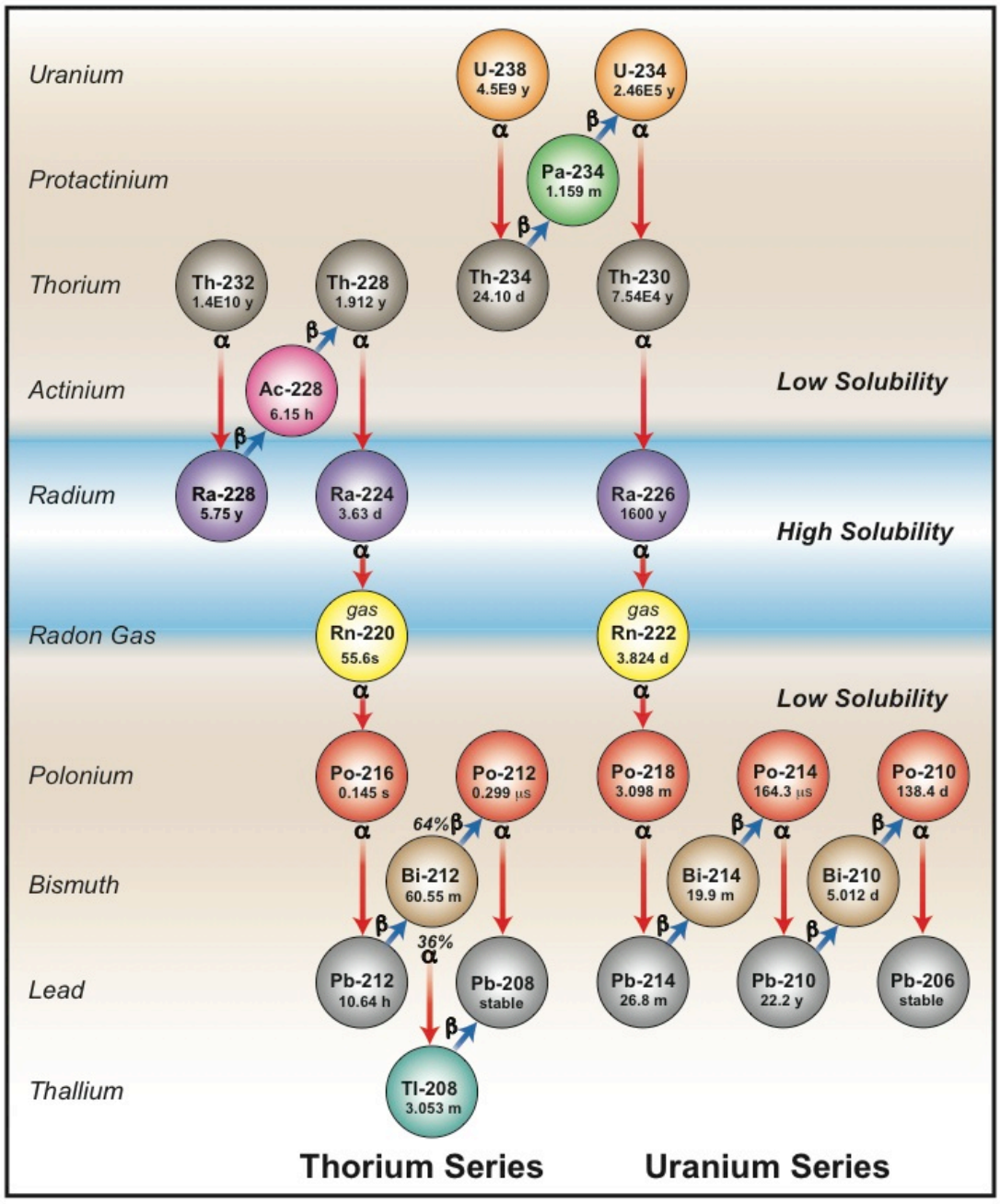
Uranium
Protactinium
Thorium
Actinium
Radium
Radon Gas
Polonium
Bismuth
Lead
Thallium
U-238
4.5E9 y
U-234
2.46E5 y
Pa-234
1.159 m
Th-234
24.10 d
Th-230
7.54E4 y
Th-232
1.4E10 y
Th-228
1.912 y
Ac-228
6.15 h
Ra-228
5.75 y
Ra-224
3.63 d
Ra-226
1600 y
gas
Rn-220
55.6s
gas
Rn-222
3.824 d
Po-216
0.145 s
Po-212
0.299 µs
Po-218
3.098 m
Po-214
164.3 µs
Po-210
138.4 d
Bi-212
60.55 m
Bi-214
19.9 m
Bi-210
5.012 d
Pb-212
10.64 h
Pb-208
stable
Pb-214
26.8 m
Pb-210
22.2 y
Pb-206
stable
Tl-208
3.053 m
64%
36%
Low Solubility
High Solubility
Low Solubility
Thorium Series
Uranium Series

Figure 2.

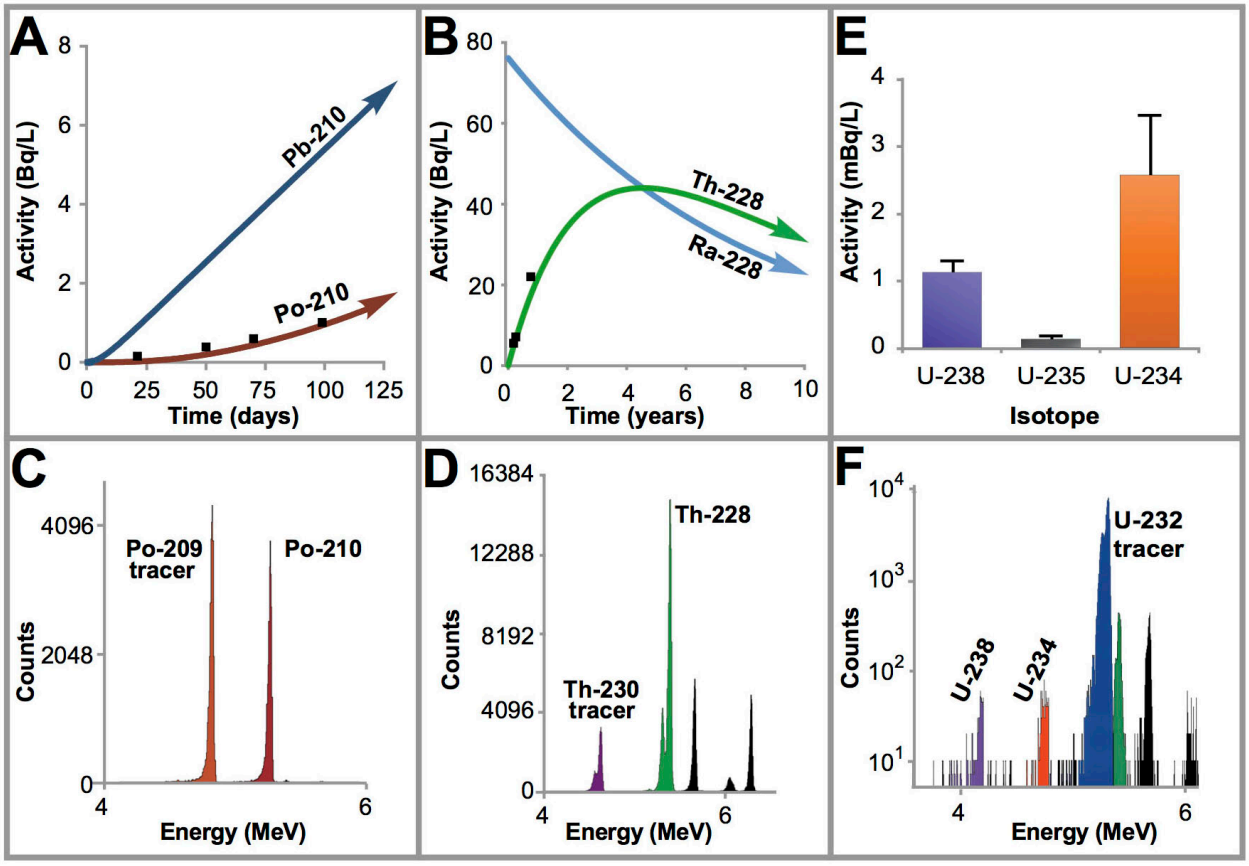
A
Activity (Bq/L)
Pb-210
Po-210
Time (days)
B
Activity (Bq/L)
Th-228
Ra-228
Time (years)
E
Activity (mBq/L)
U-238
U-235
U-234
Isotope
C
Counts
Po-209 tracer
Po-210
Energy (MeV)
D
Counts
Th-228
Th-230 tracer
Energy (MeV)
F
Counts
U-238
U-234
U-232 tracer
Energy (MeV)

Figure 3.

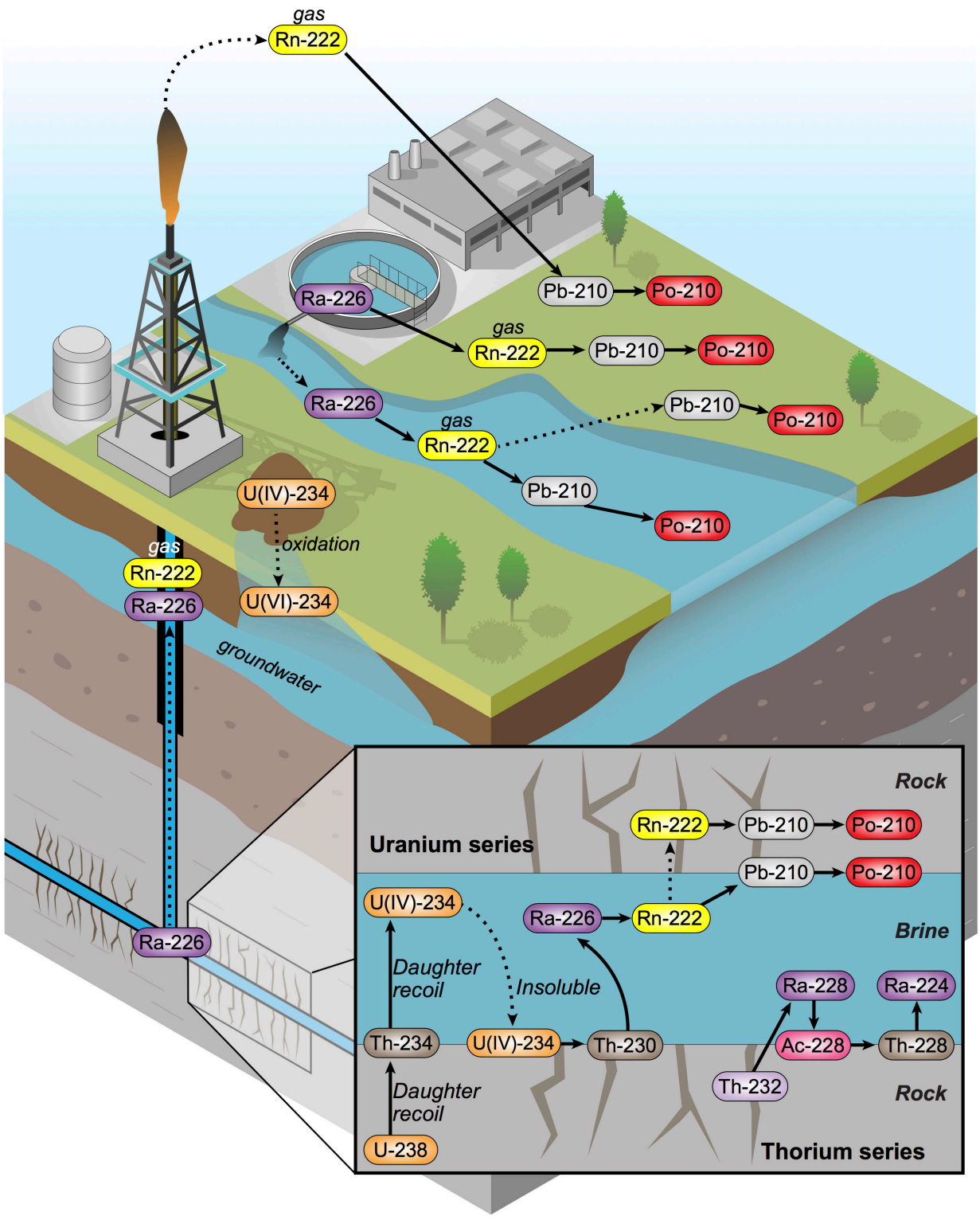
gas
Rn-222
Pb-210
Po-210
Ra-226
gas
Rn-222
Pb-210
Po-210
Ra-226
gas
Rn-222
Pb-210
Po-210
Pb-210
Po-210
U(IV)-234
oxidation
gas
Rn-222
Ra-226
U(VI)-234
groundwater
Ra-226
Rock
Uranium series
Rn-222
Pb-210
Po-210
Pb-210
Po-210
U(IV)-234
Ra-226
Rn-222
Brine
Daughter recoil
Insoluble
Ra-228
Ra-224
Th-234
U(IV)-234
Th-230
Ac-228
Th-228
Th-232
Rock
Daughter recoil
U-238
Thorium series

Figure 4.

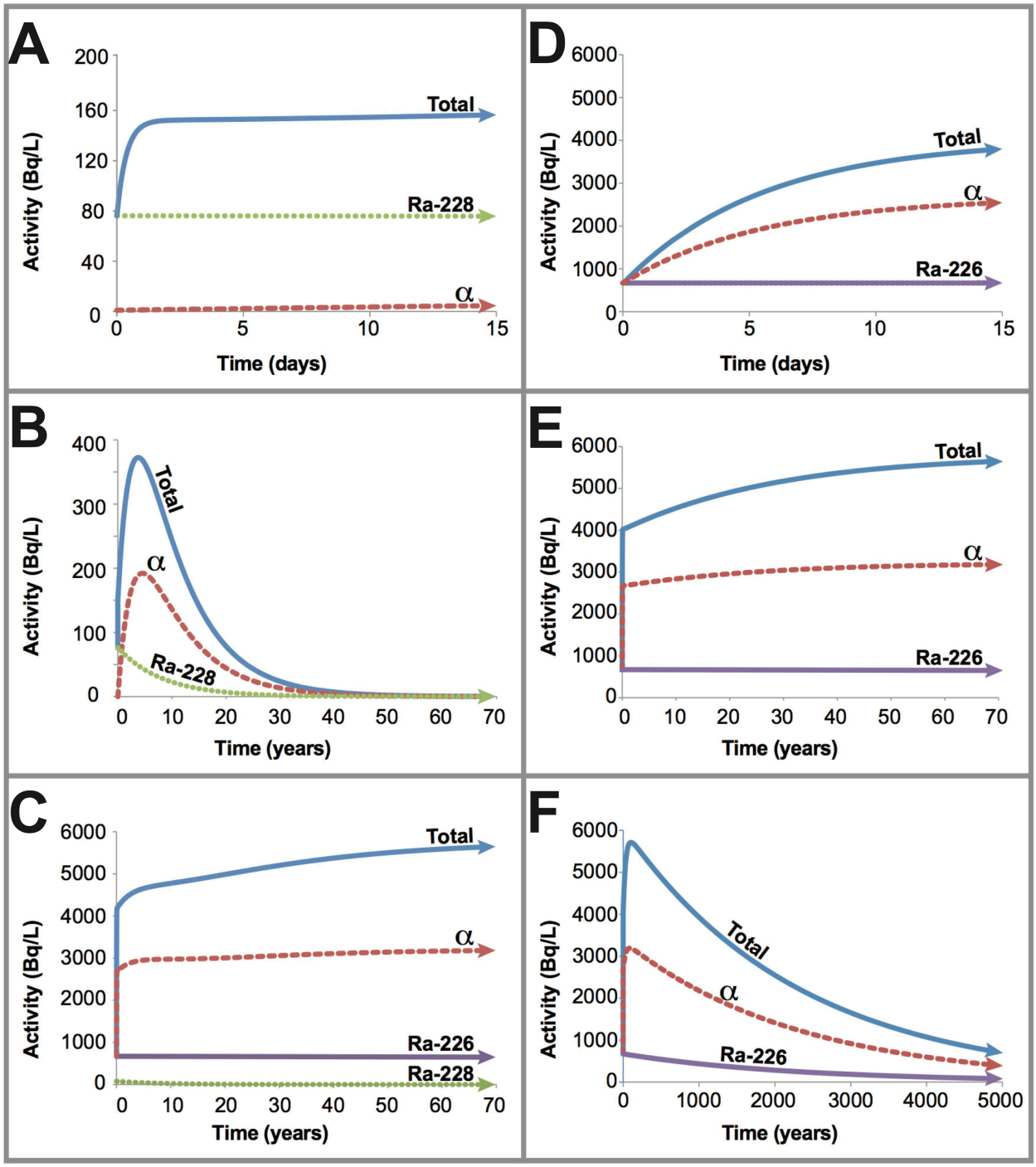
A
Activity (Bq/L)
200
160
120
80
40
0
Total
Ra-228
α
0
5
10
15
Time (days)
D
Activity (Bq/L)
6000
5000
4000
3000
2000
1000
0
Total
α
Ra-226
0
5
10
15
Time (days)
B
Activity (Bq/L)
400
300
200
100
0
Total
α
Ra-228
0
10
20
30
40
50
60
70
Time (years)
E
Activity (Bq/L)
6000
5000
4000
3000
2000
1000
0
Total
α
Ra-226
0
10
20
30
40
50
60
70
Time (years)
C
Activity (Bq/L)
6000
5000
4000
3000
2000
1000
0
Total
α
Ra-226
Ra-228
0
10
20
30
40
50
60
70
Time (years)
F
Activity (Bq/L)
6000
5000
4000
3000
2000
1000
0
Total
α
Ra-226
0
1000
2000
3000
4000
5000
Time (years)